Medical Research Archives

European Society of Medicine

OPEN ACCESS

Published: January 31, 2024

Citation: Hu, Y., et al., 2024. Preparation, and antibacterial activity of chitosan derivative containing double quaternary ammonium salt and hydantoin structures. Medical Research Archives, [online] 12(1). https://doi.org/10.18103/mra.v12i1.5108

DOI: https://doi.org/10.18103/mra.v12i1.5108

ISSN: 2375-1924

RESEARCH ARTICLE

Preparation, and antibacterial activity of chitosan derivative containing double quaternary ammonium salt and hydantoin structures

Yiting Hu[1,2], Xiaojiang Xie[1,2], Jingwei He[1,2], Fang Liu[1,2*]

[1]College of Materials Science and Engineering, South China University of Technology, No. 381, Wushan Road, Tianhe District, Guangzhou, 510640, People's Republic of China

[2]Key Lab of Guangdong Province for High Property and Functional Macromolecular Materials, South China University of Technology, No. 381, Wushan Road, Tianhe District, Guangzhou, 510640, People's Republic of China

*mcfliu@scut.edu.cn

ABSTRACT

Chitosan quaternary ammonium salt antibacterial agents with a single structure have the drawbacks of slow bactericidal speed and poor bactericidal effect, which cannot meet the practical usage requirements. To address the problem, in this study, we designed and synthesized a novel chitosan derivative containing double quaternary ammonium salt and chloride hydantoin structures (QCS-CA-DEADH-Cl) by using chitosan, 5,5-dimethyl hydantoin, methyl iodide, and 2-Dimethylaminoethyl chloride hydrochloride as the main raw materials, and then used as antibacterial agent. The structure of QCS-CA-DEADH-Cl was characterized by Fourier transform infrared spectra, X-ray photoelectron spectroscopy, Thermogravimetric, and Scanning electron microscopy. The antibacterial activity of QCS-CA-DEADH-Cl, and the renewability and stability of N-Cl structure in QCS-CA-DEADH-Cl were explored. The results indicated that the N-Cl structure of QCS-CA-DEADH-Cl has strong renewability and storage stability. Moreover, the synergistic effect of quaternary ammonium salt structure and N-Cl structure endowed QCS-CA-DEADH-Cl with excellent antibacterial activity. This work does not only provide a new perspective for the preparation of novel chitosan antibacterial agents but also contributes to expanding the comprehensive utilization of biomass resources.

Keywords: chitosan derivatives, antibacterial activity, synthesis, quaternary ammonium salt, hydantoin structure

INTRODUCTION

Chitosan, (1-4)-2-amino-2-deoxy-β-D-glucan, is the only alkaline polysaccharide in nature, which is the second abundant natural resource next to cellulose.[1-2] Chitosan has drawn a lot of attention in many fields due to its superior biocompatibility, biodegradation, and non-toxic, such as food packaging, drug delivery, and sewage treatment.[3-4] Although chitosan exhibits certain antibacterial effects, its effect is weaker.[5] In addition, the poor solubility of chitosan under neutral and alkaline conditions also limits its further application.[6] To improve the antibacterial activity and solubility of chitosan, it is usually necessary to graft the functional groups using the amine groups (-NH_2) and the hydroxyl groups (-OH) of the chitosan skeleton.[7-8]

Quaternary ammonium salt antibacterial agents have the advantage of low toxicity and long-lasting antibacterial activity.[9] Due to the presence of active -NH_2 groups in the structure of chitosan, most of its antibacterial modifications are quaternization modifications at present.[10] Although the bactericidal effect has been significantly improved by converting the amino groups on chitosan into quaternary ammonium salt structures, there are still many problems such as slow bactericidal speed and not outstanding bactericidal effects.[11] Moreover, due to the excessive use of quaternary ammonium salt antibacterial agents in recent years, some bacteria have developed resistance to them, and chitosan antibacterial agents with single quaternary ammonium cannot meet the practical usage requirements.[12] Therefore, it is necessary to develop novel antibacterial agents with superior and long-lasting activity as well as efficient and fast sterilization rates.

N-halamine antibacterial agents have the characteristics of efficient and rapid sterilization, but due to the hydrophobicity of N-halamine antibacterial agents, they do not easily come into contact with bacteria quickly.[13-14] In addition, the N-halamine antibacterial groups no longer have antibacterial activities after the contact with bacteria, leading to N-halamine antibacterial agents showing poor antibacterial persistence. Based on these knowledge, by utilizing the persistence of quaternary ammonium salt antibacterial groups, and the rapid sterilization advantages of N-halamine antibacterial groups as well as the synergistic antibacterial effect between these two antibacterial groups, it is possible to prepare chitosan antibacterial agents containing both quaternary ammonium groups and N-halamine antibacterial groups with superior antibacterial activity and efficient sterilization rates.

In this work, a novel chitosan derivative containing double quaternary ammonium salt and chloride hydantoin structures (QCS-CA-DEADH-Cl) was designed and synthesized by using chitosan (CS), 5,5-dimethyl hydantoin (DMH), methyl iodide, and 2-Dimethylaminoethyl chloride hydrochloride as the main raw materials, and then used as antibacterial agent. The structure of QCS-CA-DEADH-Cl was characterized by using Fourier transform infrared spectra (FTIR), X-ray photoelectron spectroscopy (XPS), Thermogravimetric (TG), and Scanning electron microscopy (SEM). The antibacterial activity of QCS-CA-DEADH-Cl, and the renewability and stability of N-Cl structure in QCS-CA-DEADH-Cl were systematically investigated.

EXPERIMENT

Materials

Chitosan (COS, 21 cps, 90% degree of deacetylation) was supplied from Shandong Laizhou Highly Bio-products Co., Ltd., China. 5,5- Dimethylhydantoin (DMH, 98%), and sodium iodide (99.5%) were provided by Aladdin Technology Co., Ltd., Shanghai, China. 2-Dimethylaminoethyl chloride hydrochloride (98%) was purchased from InnoChem Science and Technology Co., Ltd., Beijing, China. Methyl iodide (99%) was supplied from J&K Scientific Co., Ltd., Beijing, China. Chloroacetyl chloride (98%) was provided by Tokyo Chemical Industry, Japan. Sodium hypochlorite and N-methyl-2-pyrrolidone were purchased from Tianjin Damao Chemical Reagent Factory, Tianjin, China. Sodium thiosulfate (0.1mol/L in water) was supplied from Shenzhen Bolinda Technology Co., Ltd., China. *Escherichia coli* (*E. coli*) (ATCC 25922) and *Staphylococcus aureus* (*S. aureus*) (ATCC 6538) were provided by Shanghai Luwei Technology Co., Ltd, Shanghai, China. Nutrient agar and PBS buffer were purchased from Guangdong Huankai Microbial Technology Co., Ltd, China.

Synthesis of chitosan derivative containing double quaternary ammonium salt and hydantoin structures QCS-CA-DEADH-Cl

The synthesis route of QCS-CA-DEADH-Cl is mainly divided into the following three steps.

Step (i) The synthesis of 3-dimethylaminoethyl-5,5-dimethylhydantoin DEADH (**Fig.1**)

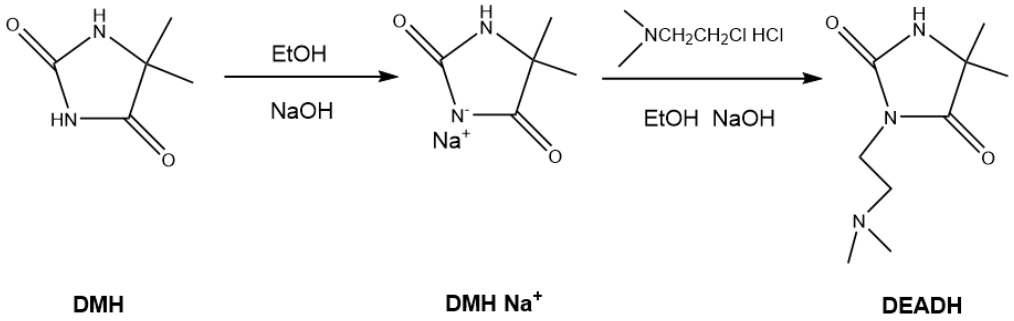

Fig. 1. The synthesis route of DEADH.

Firstly, 6.40 g of 5,5-dimethylhydantoin (DMH) and 2.00 g of sodium hydroxide were added into 50 mL of absolute alcohol. After reacting for 30 min, the dry sodium hydantoin salt (DMH Na^+) was obtained by removing the solvent with a rotary evaporator. Subsequently, 7.20 g of 2-dimethylaminoethyl chloride hydrochloride and 2.00 g of sodium hydroxide were added into 50 mL of absolute alcohol. The mixture was reacted for 30 min under ice bath, and then remove NaCl by reducing pressure filtration and collecting the filtrate. Afterward, 7.50 g of sodium hydantoin salt (DMH Na^+) was added to the collected filtrate and then stirred at 60 °C for 24 h. After the reaction was completed, the filtrate was

collected through filtration. Then, the crude product of 3-dimethylaminoethyl-5,5-dimethylhydantoin (DEADH) was obtained by removing the solvent with a rotary evaporator.[15] Finally, the obtained crude product of DEADH was further purified. The crude product of DEADH was dissolved into dichloromethane, and then collected the filtrate by filtration. The purified DEADH was acquired by removing the solvent with a rotary evaporator and drying in a vacuum oven at 60 °C.

Step (ii) The synthesis of chitosan derivative containing double quaternary ammonium salt and hydantoin structures QCS-CA-DEADH (Fig.2)

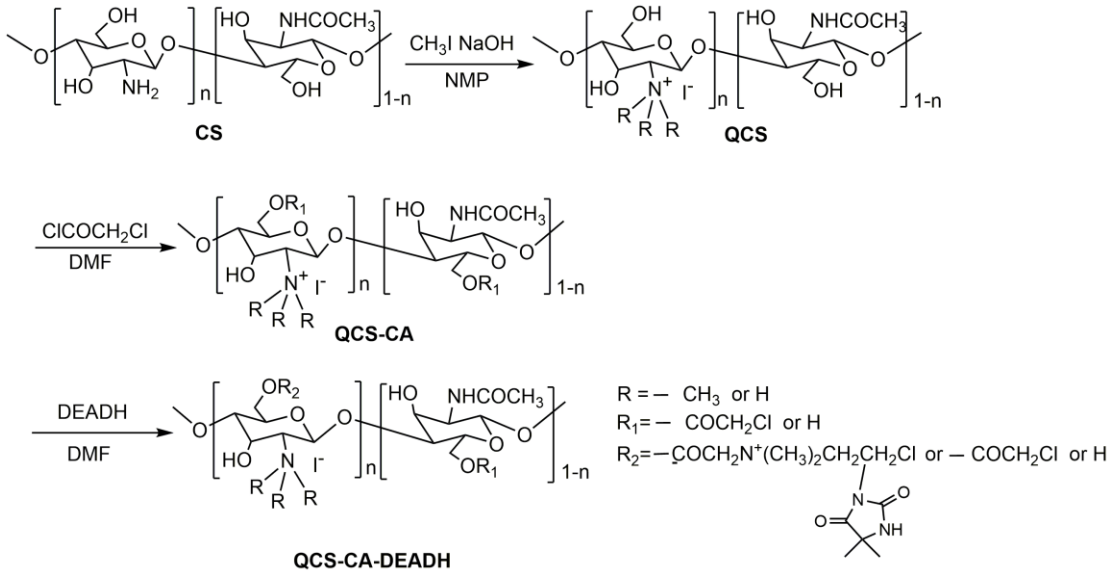

Fig. 2. The synthesis route of QCS-CA-DEADH.

2.00 g of chitosan (CS) and 100 mL of N-methyl-2-pyrrolidone were added into a 250 mL brown three-necked flask and then stirred at 50 °C for 12 h. Afterward, 10.22 g of methyl iodide, 1.80 g of sodium iodide, 1.44 g of sodium hydroxide, and 4.32 g of deionized water were added into the above CS suspension and then stirred at 60 °C for 60 h. After the reaction was completed, the reaction solution was added dropwise into acetone to acquire the solid product. Then, the solid product was washed with acetone several times and dried in a vacuum oven to obtain chitosan quaternary ammonium salt (QCS).

1.00 g of QCS was dissolved in 50 mL of N, N-dimethylformamide (DMF), and then 2.5 mL of chloroacetyl chloride ($ClCOCH_2Cl$) was added into the solution. The mixture was reacted for 2 h under ice bath, and then reacted for another 12 h at 30 °C. After the reaction was completed, the solid product was washed with acetone several times and dried in a vacuum oven to acquire chitosan quaternary ammonium salt chloroethyl ester (QCS-CA).

1.00 g of QCS-CA and 10 mL of DMF were added into a 100 mL three-necked flask and then stirred to obtain QCS-CA

suspension. 4.00 g of DEADH was dissolved into 30 mL DMF and then added to the above QCS-CA suspension. The mixture was reacted for 36 h at 60 °C. After the reaction was completed, the precipitate was filtered and washed with acetone. Then, the purified product was dried in a vacuum oven to obtain chitosan derivative containing double quaternary ammonium salt and hydantoin structures (QCS-CA-DEADH).

Step (iii) The synthesis of chitosan derivative containing double quaternary ammonium salt and chloride hydantoin structures QCS-CA-DEADH-Cl (**Fig.3**)

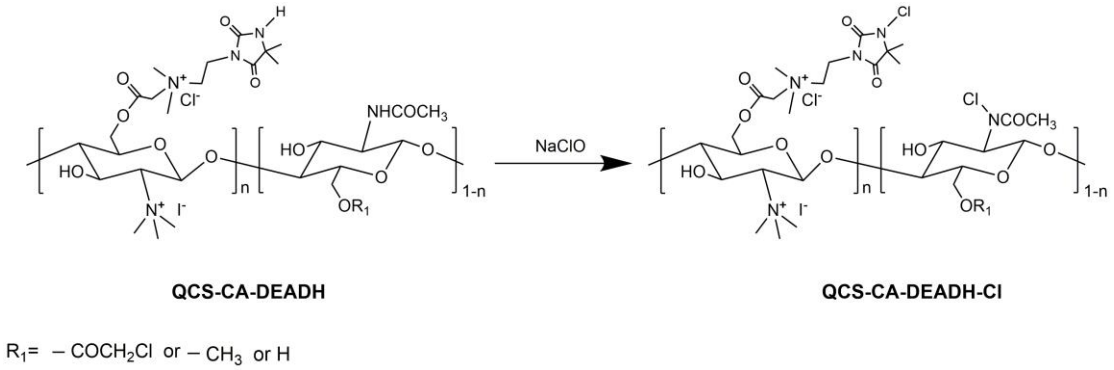

Fig. 3. The synthesis route of QCS-CA-DEADH-Cl.

1.00 g of QCS-CA-DEADH was added into 50 mL of sodium hypochlorite solution with a mass fraction of 5% and pH value of 7. The mixture was stirred for 30 min at room temperature. After the reaction was completed, the precipitate was filtered and washed with deionized water. Then, the purified product was dried in a vacuum oven to obtain chitosan derivative containing double quaternary ammonium salt and chloride hydantoin structures (QCS-CA-DEADH-Cl).

Characterization and measurements

The Fourier transform infrared spectra (FTIR) of CS, QCS, QCS-CA, QCS-CA-DEADH, and QCS-CA-DEADH-Cl were obtained from a Vector 33 FTIR spectrometer (Bruker, Germany) in the range of 600-4000 cm^{-1}. The resolution was 4 cm^{-1}, and each spectrum was scanned 32 times.

The X-ray photoelectron spectroscopy (XPS) analysis of CS and QCS-CA-DEADH-Cl was carried out on an ESCALAB XI^{+} X-ray photoelectron spectrometer (Thermo Scientific, Germany) with the Al Kα source (1486.6 eV). The operating voltage was 15 kV, and the operating current was 10 mA.

The morphology of CS, QCS-CA-DEADH, and QCS-CA-DEADH-Cl were performed with a Merlin scanning electron microscopy (SEM) (Zeiss, Germany). The acceleration voltage of the electron beam was 5 kV.

The thermal stabilities of CS, QCS, QCS-CA, QCS-CA-DEADH, and QCS-CA-DEADH-Cl were tested on a thermogravimetric instrument (TG 209 F1, Netzsch, Germany) under nitrogen atmosphere. The heating rate was 10 °C/min, and the temperature range was from 35 °C to 700 °C.

The elemental content of CS, QCS, QCS-CA, and QCS-CA-DEADH was tested by using an elemental analyzer (Vario EL cube, Elementar, Germany). The degree of substitution (DS) of the samples was obtained based on the following equation (1).[16]

$$DS=(b-a)/(X-bY) \quad (1)$$

where a is the ratio of the number of C and N atoms of chitosan reactants in the same reaction, b is the ratio of the number of C and N atoms of chitosan products in the same reaction, X, Y is the number of C and N atoms of grafted small molecular compounds, respectively.

The content of active chlorine (Cl^+%) of QCS-CA-DEADH-CL was tested by using iodometric titration. 0.10 g of QCS-CA-DEADH-Cl powder was added into 20 mL of saturated potassium iodide solution. Then, 0.1 mol/L of sodium thiosulfate standard solution was dropped into the above solution until colorless. The content of active chlorine (Cl^+%) of QCS-CA-DEADH-CL was calculated by using the following equation (2).[17]

$$Cl^+\%=(N\times V\times 34.45)\times 100\%/(2\times W) \quad (2)$$

where N and V stand for the molar concentration (mol/L) and consumed solution volume (L) of sodium thiosulfate standard solution used for titration, respectively, W stands for the mass of the sample.

The renewability of active chlorine in QCS-CA-DEADH-Cl was tested based on iodometric titration. The active chlorine content after chlorination of QCS-CA-DEADH into QCS-CA-DEADH-Cl was obtained by using iodometric titration. QCS-CA-DEADH-Cl was added into the excess of 0.1mol/L sodium thiosulfate standard solution and then stirred at room temperature for 30 min to completely quench the active chlorine. Afterward, the mixture was filtered and the unreacted sodium thiosulfate was removed with deionized water. Then, QCS-CA-DEADH was chlorinated again by using the sodium hypochlorite solution. The same process of quenching and chlorination was repeated 10 times. The active chlorine content in QCS-CA-DEADH-Cl after each chlorination was detected by using the above iodine titration method.

The storage stability of N-Cl structure in QCS-CA-DEADH-Cl was tested based on the following steps. QCS-CA-DEADH-Cl was stored in a dryer for 28 days, and the content of active chlorine of QCS-CA-DEADH-Cl was determined every 7 days.

The antibacterial efficiencies of CS, QCS, QCS-CA, QCS-CA-DEADH, and QCS-CA-DEADH-Cl toward *Escherichia coli* (*E. coli*) (ATCC 25922) and *Staphylococcus aureus* (*S. aureus*) (ATCC 6538) were tested according to ISO 22196-2011. 0.1 g of sample, 5 mL sterile PBS solution, and 5 mL bacterial suspension with a concentration of approximately 1×10^9 CFU/mL were added in turn to a 15 mL sterilized centrifuge tube. Then, the centrifuge tube was placed in a constant temperature incubator at 37 °C for cultivation. After contacting between bacteria and sample for 1 min, 5 min, 10 min, and 30 min, respectively, absorbed 500 μL upper layer bacterial solution with a pipette and then added into a centrifuge tube containing 2 mL of sodium thiosulfate standard solution with a concentration of 0.10 mol/L. After mixing evenly, dropped 100 μL the above solution onto a 96-well cell culture plate and then used sterile PBS solution to dilute it. Afterward, selected the diluent with an appropriate

dilution ratio and then dropped 20 μL the diluent into the solid LB agar medium. Subsequently, the bacterial solution was applied evenly onto the culture medium by using a sterilized coating rod. Finally, counted the colonies on the culture medium after incubated in a constant temperature incubator at 37 °C for 24 h. The number of bacteria reduced (Log value) was calculated according to the following equation (3):

$$Log=lg(B/A) \quad (3)$$

Where A is the average number of bacteria after vaccination, B is the average number of bacteria before vaccination.

RESULTS

FTIR results

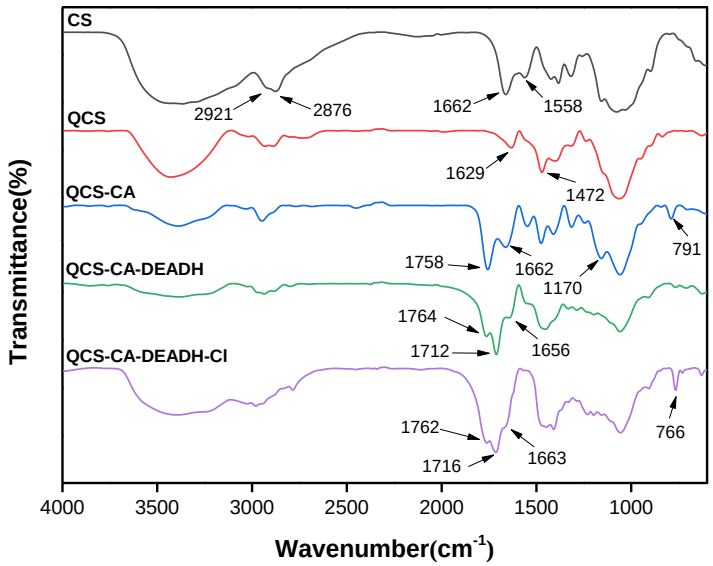

Fig. 4. FTIR spectra of CS, QCS, QCS-CA, QCS-CA-DEADH, and QCS-CA-DEADH-Cl.

Fig. 4 displays the FTIR spectra of CS, QCS, QCS-CA, QCS-CA-DEADH, and QCS-CA-DEADH-Cl. As shown in **Fig. 4**, COS presents the characteristic absorption peaks at 1662 and 1558 cm^{-1}. Compared to the spectrum of the COS, there are new peaks at 1472 cm^{-1} in the spectrum of the QCOS. In the spectrum of QCS-CA, new peaks appear at 1785, 1170, and 791 cm^{-1} compared to QCS. In addition, in the spectrum of QCS-CA-DEADH, new peaks appear at 1764 and 1712 cm^{-1} and the absorption peak of C-Cl at 791 cm^{-1} disappears compared to QCS-CA. Moreover, compared to the spectrum of QCS-CA-DEADH, the new characteristic absorption peaks appear at 767 cm^{-1} in the spectrum of QCS-CA-DEADH-Cl.

Elemental analysis results

Table 1 The results of the elemental analysis of CS, QCS, QCS-CA, and QCS-CA-DEADH.

Samples	Found			DS
	C%	N%	H%	
CS	48.50	7.51	6.598	/
QCS	22.43	3.12	6.224	0.853
QCS-CA	39.43	4.61	6.584	0.796
QCS-CA-DEADH	45.39	9.32	7.453	0.534

Table 1 lists the results of the elemental analysis of CS, QCS, QCS-CA, and QCS-CA-DEADH. It can be seen from **Table 1** that the degree of substitution (DS) of QCS, QCS-CA, and QCS-CA-DEADH is 0.853, 0.796, and 0.534, respectively.

XPS results

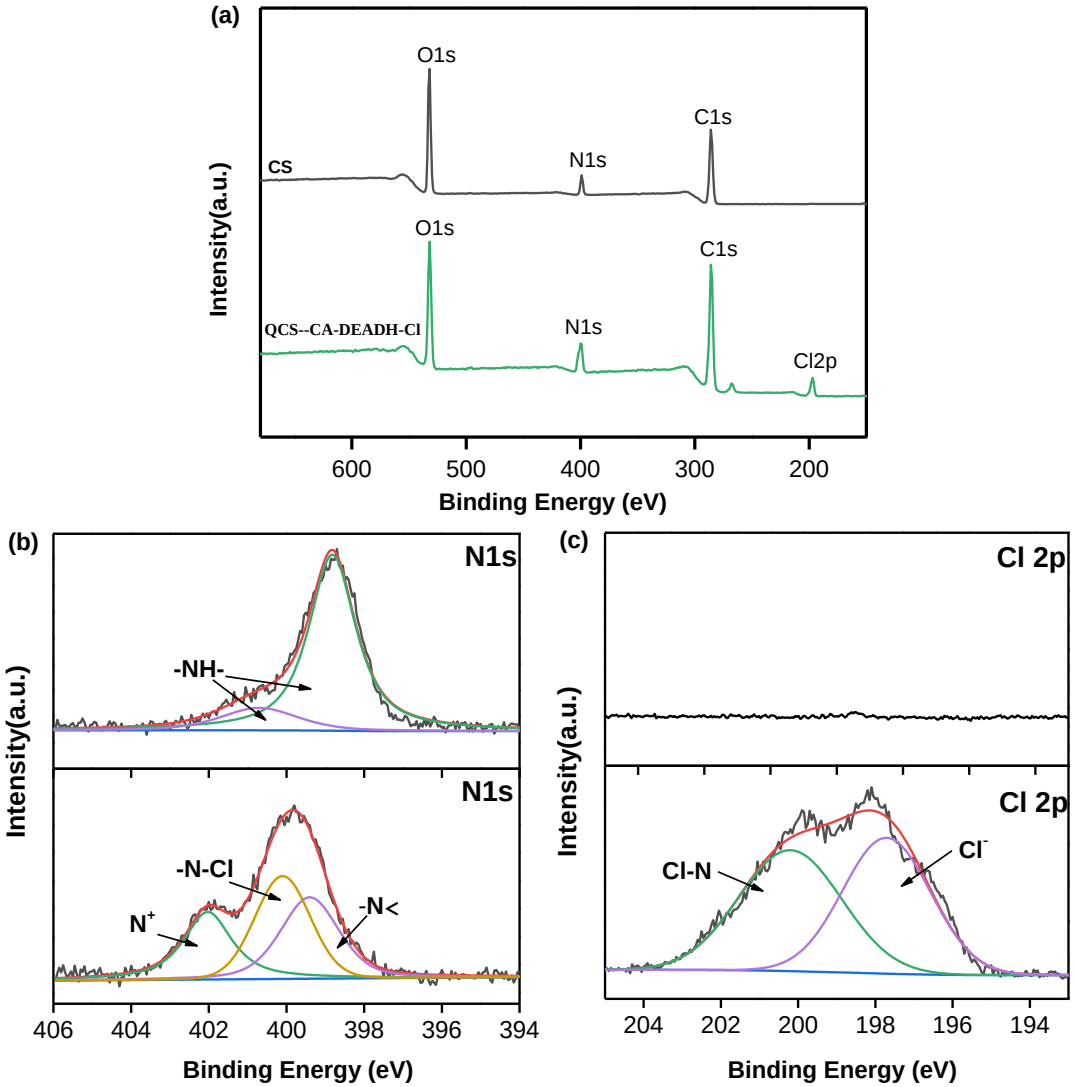

Fig. 5. (a) The whole XPS spectra of CS and QCS-CA-DEADH-Cl, (b) The high-resolution XPS survey of N1s for CS and QCS-CA-DEADH-Cl, (c) The high-resolution XPS survey of Cl2p for CS and QCS-CA-DEADH-Cl.

Fig. 5 shows the XPS spectra of CS and QCS-CA-DEADH-Cl. As shown in Fig. 5 (a), compared to the whole XPS spectra of CS, in the spectra of QCS-CA-DEADH-Cl appears the binding energy peaks of Cl2p in the range of 190 to 210 eV. In addition, it can be seen from Fig. 5 (b) that the absorption peak of N1s in CS can be divided into two peaks. These two peaks are located at 398.82 eV and 400.7 eV, respectively. Meanwhile, the absorption peak of N1s for QCS-CA-DEADH-Cl is divided into three peaks, which are located at 399.40 eV, 400.10 eV, and 402.01 eV, respectively. Moreover, as illustrated in Fig. 5 (c), the absorption peak of Cl2p for QCS-CA-DEADH-Cl is divided into two peaks. These two peaks are located at 197.71 eV and 200.20 eV, respectively.

TG results

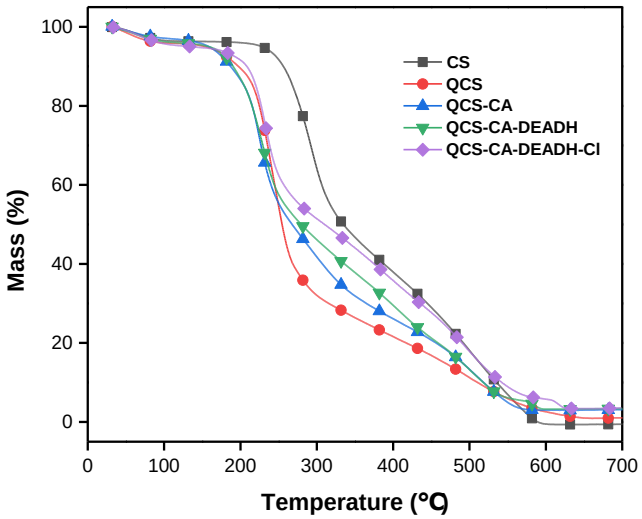

Fig. 6. The TG curves of CS, QCS, QCS-CA, QCS-CA-DEADH, and QCS-CA-DEADH-Cl in N_2 atmosphere.

Table 2 TG characteristic parameters of CS, QCS, QCS-CA, QCS-CA-DEADH, and QCS-CA-DEADH-Cl in N_2 atmosphere.

Samples	[a]T_{onset} (℃)	[b]T_{max} (℃)
CS	228.8	293.0
QCS	183.6	241.4
QCS-CA	151.6	225.3
QCS-CA-DEADH	177.0	230.0
QCS-CA-DEADH-Cl	171.5	227.8

[a] T_{onset} refers to the initial temperature of chitosan and chitosan derivatives decomposition.
[b] T_{max} refers to the temperature when the DTG curve reaches the maximum value.

Fig. 6 displays the TG curves of CS, QCS, QCS-CA, QCS-CA-DEADH, and QCS-CA-DEADH-Cl, and the related TG characteristic parameters obtained from TG curves are listed in Table 2. It can be seen from Fig. 6 that CS and chitosan derivatives QCS, QCS-CA, QCS-CA-DEADH, and QCS-CA-DEADH-Cl all exhibit a significant weight loss at 100.0 °C. In addition, as shown in Table 2, the value of T_{onset} and T_{max} of CS in N_2 atmosphere is 228.8 °C and 293.0 °C, respectively. Meanwhile, the value of T_{onset} and T_{max} of chitosan derivatives QCS, QCS-CA, QCS-CA-DEADH, and QCS-CA-DEADH-Cl are all lower than that of CS. Compared to QCS, and QCS-CA, the value of T_{onset} and T_{max} of QCS-CA-DEADH all have a significant increase. It is worth noting that the values of T_{onset} and T_{max} of QCS-CA-DEADH-Cl are all lower than that of QCS-CA-DEADH.

SEM results

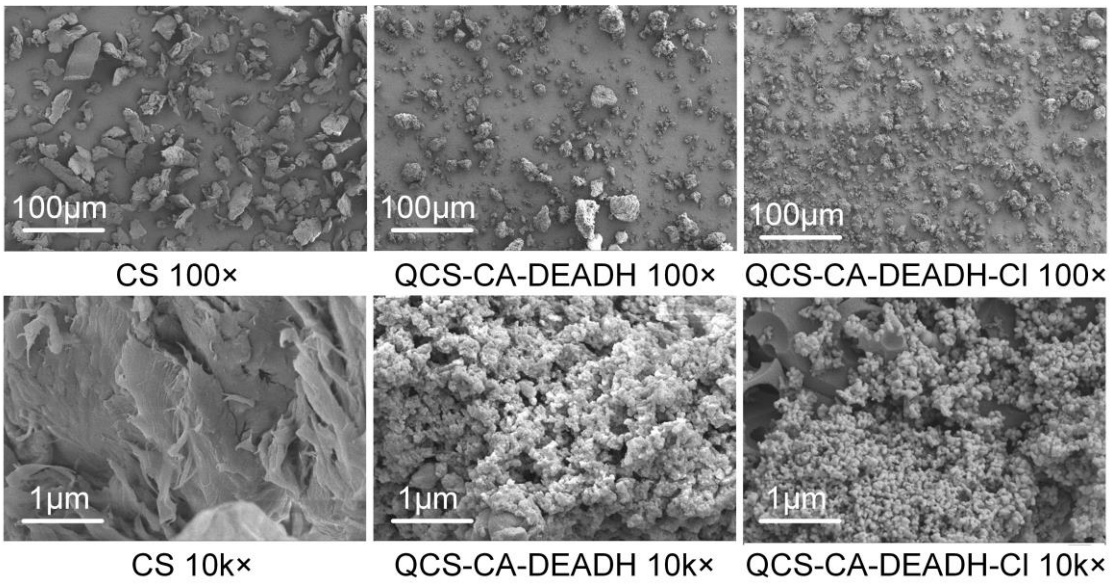

Fig. 7. SEM images of CS, QCS-CA-DEADH, and QCS-CA-DEADH-Cl.

Fig. 7 shows the SEM images of CS, QCS-CA-DEADH, and QCS-CA-DEADH-Cl. As shown in Fig. 7, chitosan before modification appears as layered fibrous structure, and its surface contains a large number of protruding microfibers. Meanwhile, the modified chitosan derivatives QCS-CA-DEADH, and QCS-CA-DEADH-Cl are all loose block-shaped particles. The surface of QCS-CA-DEADH, and QCS-CA-DEADH-Cl is rough and porous. In addition, compared to QCS-CA-DEADH, the surface of QCS-CA-DEADH-Cl becomes rougher.

Antibacterial activities

Table 3 Antibacterial activities of CS, QCS, QCS-CA-DEADH, and QCS-CA-DEADH-Cl against *E. coli* and *S. aureus*.

Samples	Contact time (min)	Log reduction	
		E. coli [a]	*S. aureus* [b]
CS	1	0.018	0.064
	5	0.155	0.101
	10	0.222	0.120
	30	0.317	0.184
QCS	1	1.453	1.763
	5	2.507	1.985
	10	2.632	2.161
	30	2.808	2.462
QCS-CA-DEADH	1	0.361	0.120
	5	0.486	0.184
	10	0.507	0.207
	30	0.528	0.286
QCS-CA-DEADH-Cl	1	9.206	8.860
	5	9.206	8.860
	10	9.206	8.860
	30	9.206	8.860

[a] The inoculum population was 1.607×10^9 (9.206 log) CFU/sample.

[b] The inoculum population was 7.244×10^8 (8.860 log) CFU/sample.

Table 3 shows the results of the antibacterial activities of CS, QCS, QCS-CA-DEADH, and QCS-CA-DEADH-Cl against *E. coli* and *S. aureus*. It can be seen from **Table 3** that the Log values of *E. coli* and *S. aureus* only reached 0.317 and 0.184 after 30 min of contact time with CS, respectively. In addition, the Log value of *E. coli* and *S. aureus* after 1 min of contact time with QCS is 1.453 and 1.763, respectively, which is significantly higher than the Log value of *E. coli* and *S. aureus* after 30 min of contact time with CS. The Log values of *E. coli* and *S. aureus* after contact with QCS-CA-DEADH for 1 min, 5 min, 10 min, and 30 min are all lower than the Log values of *E. coli* and *S. aureus* after contact with QCS. It is worth noting that the Log values of *E. coli* and *S. aureus* after contact with QCS-CA-DEADH-Cl for 1 min, 5 min, 10 min, and 30 min are all significantly higher than the Log values of *E. coli* and *S. aureus* after contact with QCS, QCS-CA, and QCS-CA-DEADH. After contact with QCS-CA-DEADH-Cl, *E. coli,* and *S. aureus* are inactivated within 1 min.

Renewability and stability of N-Cl structure in QCS-CA-DEADH-Cl

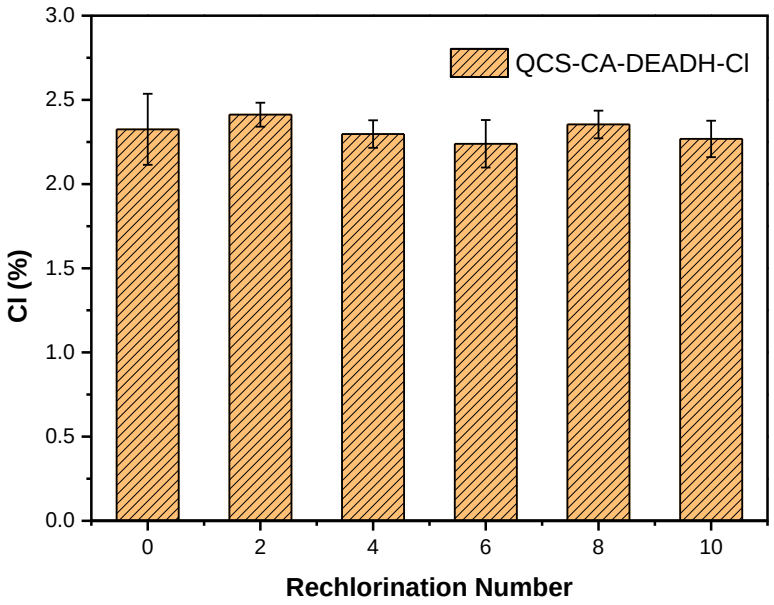

Fig. 8. The renewability of N-Cl structure in QCS-CA-DEADH-Cl.

The N-Cl structure is renewable and can be transformed into an N-H structure after being consumed. The transformed N-H structure can be reconverted into N-Cl structure after being in contact with sodium hypochlorite again.[18] To explore the renewability of the N-Cl structure in QCS-CA-DEADH-Cl, sodium thiosulfate is used to quench the active chlorine (N-Cl) on the QCS-CA-DEADH-Cl structure and convert it into N-H, then sodium hypochlorite is used to chlorinate N-H into active chlorine (N-Cl). Afterward, the renewability of N-Cl structure in QCS-CA-DEADH-Cl is evaluated by measuring the changes in their active chlorine content using the iodine titration method. Fig. 8 shows the changes in the active chlorine content of QCS-CA-DEADH-Cl after multiple quenching-chlorination treatments. It can be seen from Fig. 8 that the active chlorine content of QCS-CA-DEADH-Cl remains basically unchanged after 10 quenching-chlorination treatments.

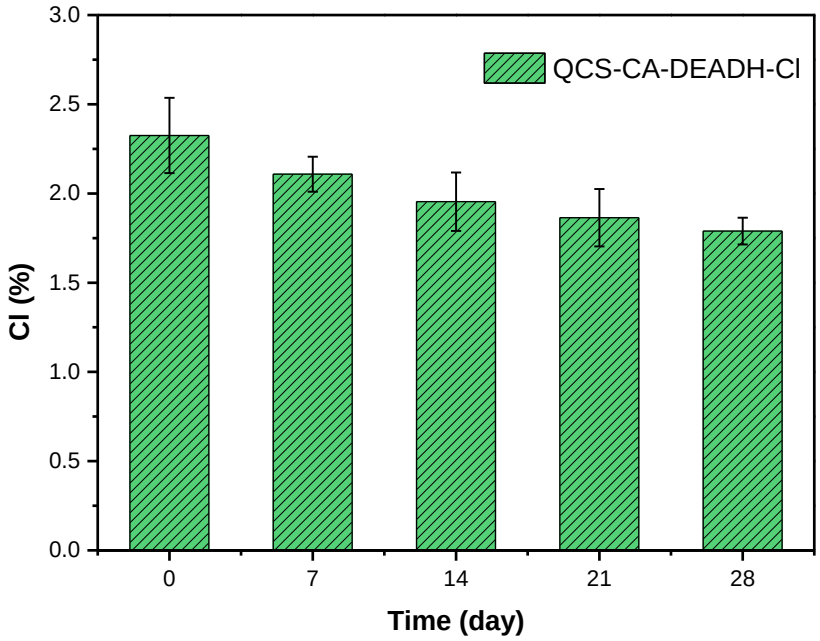

Fig. 9. The storage stability of N-Cl structure in QCS-CA-DEADH-Cl.

The storage stability of N-Cl structure in QCS-CA-DEADH-Cl is investigated by recording the changes in active chlorine of QCS-CA-DEADH-Cl after being stored at room temperature for 28 days. Fig. 9 shows the results of the storage stability test of N-Cl structure in QCS-CA-DEADH-Cl. As displayed in Fig. 9, the active chlorine content in QCS-CA-DEADH-Cl remains above 70% after 28 days of storage.

DISCUSSION

In the FTIR spectra (Fig. 4) of QCS, the new peaks at 1472 cm^{-1} are assigned to the stretch vibration of C-H groups of $-N^{+}(CH_3)_3$ structure, indicating that the amino groups of CS have successfully undergone the quaternization reaction.[19] In the FTIR spectra of QCS-CA, new peaks appear at 1785, 1170, and 791 cm^{-1} compared to QCS, which correspond to the stretch vibration of C=O and C-O groups in alkyl esters and the stretch vibration of C-Cl groups, respectively, indicating that $ClCOCH_2Cl$ has successfully reacted with the -OH groups at the C6 position in QCS. In addition, in the FTIR spectra of QCS-CA-DEADH, new peaks appear at 1764 and 1712 cm^{-1} compared to QCS-CA, which originates from the stretching vibration of the imine carbonyl and urea carbonyl groups in the hydantoin structure, respectively. Meanwhile, the absorption peak of C-Cl at 791 cm^{-1} disappears, implying that DEADH has been successfully introduced into QCS-CA by reacting with chloroalkanes of QCS-CA. Moreover, compared to the spectrum of QCS-CA-DEADH, the characteristic absorption peaks of N-Cl groups in QCS-CA-DEADH-Cl occur at 767 cm^{-1}, suggesting that QCS-CA-DEADH-Cl has been successfully prepared.[20]

The results of the elemental analysis (Table 1) indicate that the degree of substitution (DS) of QCS-CA-DEADH is 0.534, which is much higher than the degree of substitution reported in the literature for directly grafting cyclic halogenated amine structures onto chitosan.[21-22]

In the XPS spectra (**Fig. 5**) of CS, the absorption peaks of N1s at 398.82 eV and 400.7 eV belong to the -NH- structure of the amino and amide groups, respectively.[23] In the high-resolution XPS survey of N1s for QCS-CA-DEADH-Cl, the amide nitrogen (-N<) appears at 399.40 eV, the amide nitrogen appears at 400.10 eV, and the quaternary ammonium salt nitrogen (N^+) appears at 402.01 eV, indicating that QCS-CA-DEADH-Cl not only contains quaternary ammonium structure but also contains hydantoin structure.[24] Moreover, in the high-resolution XPS survey of Cl2p for QCS-CA-DEADH-Cl, the Cl2p absorption peak of the Chloride ion appears at 197.71 eV, and the Cl2p absorption peak of N-Cl appears at 200.20 eV, implying QCS-CA-DEADH-Cl is successfully prepared.

In the TG curves (**Fig. 6**) of chitosan derivatives QCS, QCS-CA, QCS-CA-DEADH, and QCS-CA-DEADH-Cl all present a significant weight loss at 100.0 °C, which is mainly related to the water absorption of quaternary ammonium salt groups in their structure. In addition, due to the crystalline structure of chitosan being destroyed during the grafting process, resulting in the values of T_{onset} and T_{max} of chitosan derivatives QCS, QCS-CA, QCS-CA-DEADH, and QCS-CA-DEADH-Cl are lower than that of CS. The values of T_{onset} and T_{max} of QCS-CA-DEADH are all higher than that of QCS, and QCS-CA. This is mainly due to the presence of C=O and N-H structures in the grafted DEADH, which can generate hydrogen bonds between molecules. Moreover, the values of T_{onset} and T_{max} of QCS-CA-DEADH-Cl are all lower than that of QCS-CA-DEADH. This is mainly attributed to two reasons. On the one hand, the etching effect of sodium hypochlorite solution on QCS-CA-DEADH during the chlorination process further destroys the crystalline structure. On the other hand, the N-Cl structure of QCS-CA-DEADH-Cl is prone to decomposition.[25]

In the SEM images (**Fig. 7**) of QCS-CA-DEADH and QCS-CA-DEADH-Cl, their surface is rough and porous. This is due to the introduction of functional groups on the chitosan chain, which weakens the hydrogen bonds within and between chitosan molecules, destroying the original ordered crystalline structure of chitosan and thus altering its morphology.[26] In addition, the surface of QCS-CA-DEADH-Cl becomes rougher compared to QCS-CA-DEADH, which may be caused by the etching effect of active chlorine.

The above analysis results of FTIR, XPS, TG, and SEM suggest that QCS-CA-DEADH-Cl is successfully prepared.

The results of the antibacterial activities (**Table 3**) indicate that unmodified chitosan exhibits poor antibacterial activity. This is due to the unmodified chitosan has poor solubility, and its surface structure is smooth and dense, resulting in the weaker ability to penetrate bacterial cell membranes and cell walls. Unmodified chitosan can only rely on the chelation of its amino groups to bind with metal ions on the surface of bacteria, thereby affecting bacterial physiological activities, or by forming polymer films on the surface of bacteria to prevent bacterial material transport.[27] However, chelation and the formation of polymer films usually take a long time, so chitosan cannot achieve significant antibacterial effects in a short time.

The antibacterial activity of QCS is superior to that of CS. This is related to the amino quaternization of chitosan destroys the hydrogen bonds between chitosan molecules and the formation of N^+ cations endowing QCS with better water solubility.[28] Thus, QCS molecular chains can sufficiently contact with bacteria in aqueous solutions. The N^+ cations on QCS molecular chains can interact with the negative charges on the bacterial surface to generate electrostatic interactions, damaging the bacterial cell membrane and killing bacteria.

In addition, the Log values of *E. coli* and *S. aureus* after contact with QCS-CA-DEADH are all lower than the Log values of *E. coli* and *S. aureus* after contact with QCS, indicating that the introduction of hydantoin structure into QCS decreases the antibacterial activity of QCS. Although new quaternary ammonium salt structures are generated in QCS grafted with hydantoin structure, the molecular weight of the corresponding chitosan derivatives QCS-CA-DEADH also increases. Under the same quality of antibacterial agent conditions, compared to QCS, the number of moles of QCS-CA-DEADH is smaller. In addition, the antibacterial activity of quaternary ammonium salt antibacterial agents is not only related to charge density but also affected by the steric hindrance of hydrophobic chains connected to the quaternary ammonium salt structure.[29,30] Due to the steric hindrance of the hydantoin structure, the quaternary ammonium salt groups connected to the hydantoin structure are less likely to contact negative charges on the bacterial surface. Meanwhile, the hydantoin structure also weakens the hydrophilicity of QCS-CA-DEADH, making it insoluble in water and unable to stretch the molecular chains, further causing the N^+ cations of QCS-CA-DEADH are less likely to contact with bacteria. Thus, QCS-CA-DEADH shows poor antibacterial activity.

In addition, the Log values of *E. coli* and *S. aureus* after contact with QCS-CA-DEADH-Cl are all higher than the Log values of *E. coli* and *S. aureus* after contact with QCS, QCS-CA, and QCS-CA-DEADH, implying that the antibacterial activity of QCS-CA-DEADH-Cl is significantly superior to QCS, QCS-CA, and QCS-CA-DEADH. This is mainly related to QCS-CA-DEADH-Cl containing quaternary ammonium salt structure and chloride halogenated amine structure. The N^+ cations in the quaternary ammonium salt structure can attract negative charges on the bacterial surface, which promotes the contact between QCS-CA-DEADH-Cl and bacteria and forms electrostatic interaction with the cell membrane to destroy the bacterial structure. In addition, the N-Cl structure in QCS-CA-DEADH-Cl can directly oxidize the bacterial cell membrane and cell wall after QCS-CA-DEADH-Cl contacts with bacteria, destroy bacterial integrity, and transform itself into N-H structure.[31] Meanwhile, the N-Cl structure of QCS-CA-DEADH-Cl can release highly oxidizing halogen cations into the interior of bacteria after QCS-CA-DEADH-Cl contact with the aqueous solution, to damage the internal substances of bacteria. Thus, the synergistic effect of quaternary ammonium salt structure and N-Cl structure endows QCS-CA-DEADH-Cl with excellent antibacterial activity and sterilization rate.[32,33]

Renewable test results (**Fig. 8**) of active chlorine in QCS-CA-DEADH-Cl indicate that the N-Cl groups of QCS-CA-DEADH-Cl have strong renewability. After simple chlorination

treatment, the N-H structure can be transformed back into the N-Cl structure again.

The storage stability test results (**Fig. 9**) of the N-H structure in QCS-CA-DEADH-Cl suggest QCS-CA-DEADH-Cl has better storage stability. This is mainly due to the N-Cl bond being located on the amide structure of the hydantoin ring, which has higher stability than the N-Cl bond on the non-cyclic structure.

CONCLUSIONS

In this work, a novel chitosan derivative containing double quaternary ammonium salt and chloride hydantoin structures QCS-CA-DEADH-Cl was successfully prepared and then used as antibacterial agent. The synthesized QCS-CA-DEADH-Cl was characterized by using FTIR, XPS, TG, and SEM. In addition, the antibacterial activity of QCS-CA-DEADH-Cl, and the renewability and stability of N-Cl structure in QCS-CA-DEADH-Cl were explored in detail. The results of the antibacterial activity test indicated that QCS-CA-DEADH-Cl had excellent antibacterial activity and rapid bactericidal rate, which could completely inactivate *E. coil* and *S. aureus* within 1 min. Moreover, the results of renewability and stability tests of the N-Cl structure in QCS-CA-DEADH-Cl suggested that the N-Cl structure in QCS-CA-DEADH-Cl possessed superior renewability and storage stability.

DECLARATION OF COMPETING INTEREST

The authors declare that they have no known competing financial interests or personal relationships that could have appeared to influence the work reported in this paper.

ACKNOWLEDGMENTS

This work was supported by the National Natural Science Foundation of China (51973062).

FUNDING

None

References:

[1] Anitha A, Sowmya S, Kumar PTS, et al. Chitin and chitosan in selected biomedical applications. *Progress in Polymer Science*. 2014; 39(9):1644-1667.

[2] Petroni S, Tagliaro I, Antonini C, et al. Chitosan-Based Biomaterials: Insights into Chemistry, Properties, Devices, and Their Biomedical Applications. *Marine drugs*. 2023;21(3):147(1-56).

[3] Sahariah P, Benediktssdottir BE, Hjalmarsdottir MA, et al. Impact of chain length on antibacterial activity and hemocompatibility of quaternary N-alkyl and N,N-dialkyl chitosan derivatives. *Biomacromolecules*. 2015; 16(5):1449-1460.

[4] Szulc M, Lewandowska K. Biomaterials Based on Chitosan and Its Derivatives and Their Potential in Tissue Engineering and Other Biomedical Applications-A Review. *Molecules*. 2023;28(1):247(1-17).

[5] Hosseinnejad M, Jafari SM. Evaluation of Different Factors Affecting Antimicrobial Properties of Chitosan. *International Journal of Biological Macromolecules*. 2016;85:467-475.

[6] Wang L, Xin M, Li M, et al. Effect of the structure of chitosan quaternary phosphonium salt and chitosan quaternary ammonium salt on the antibacterial and antibiofilm activity. *International Journal of Biological Macromolecules*. 2023;242:124877-124874.

[7] Ding S, Wang Y, Li J, et al. Progress and prospects in chitosan derivatives: modification strategies and medical applications. *Journal of Materials Science & Technology*. 2021;89:209-224.

[8] Chen Y, Li J, Li Q, et al. Enhanced water-solubility, antibacterial activity and biocompatibility upon introducing sulfobetaine and quaternary ammonium to chitosan. *Carbohydrate Polymers*. 2016;143:246-253.

[9] Dan W, Gao J, Qi X, et al. Antibacterial quaternary ammonium agents: Chemical diversity and biological mechanism. *European Journal of Medicinal Chemistry*. 2022; 243:114765(1-12).

[10] Tabriz A, Alvi M, Niazi MBK, et al. Quaternized trimethyl functionalized chitosan based antifungal membranes for drinking water treatment. *Carbohydrate Polymers*. 2019;207:17-25.

[11] Wei L, Chen Y, Tan W, et al. Synthesis, Characterization, and Antifungal Activity of Pyridine-Based Triple Quaternized Chitosan Derivatives. *Molecules*. 2018; 23(10):2604(1-12).

[12] Oblak E, Piecuch A, Maciaszczyk-Dziubinska E, et al. Quaternary ammonium salt *N*-(dodecyloxycarboxymethyl)-*N*,*N*,*N*-trimethyl ammonium chloride induced alterations in *Saccharomyces cerevisiae* physiology. *Journal of Biosciences*. 2016; 41(4):601-614.

[13] Ren H, Du Y, Su Y, et al. A Review on Recent Achievements and Current Challenges in Antibacterial Electrospun *N*-halamines. *Colloid and Interface Science Communications*. 2018;24:24-34.

[14] Dong A, Wang Y-J, Gao Y, et al. Chemical Insights into Antibacterial N-Halamines. *Chemical Reviews*. 2017;117(6):4806-4862.

[15] Rahma H, Asghari S, Logsetty S, et al. Preparation of Hollow N-Chloramine-Functionalized Hemispherical Silica Particles with Enhanced Efficacy against Bacteria in the Presence of Organic Load: Synthesis, Characterization, and Antibacterial Activity. *Acs Applied Materials & Interfaces*. 2015; 7(21):11536-11546.

[16] Tian W, Li Q, Dong F, et al. Novel cationic chitosan derivative bearing 1,2,3-triazolium and pyridinium: Synthesis, characterization, and antifungal property. *Carbohydrate Polymers*. 2018;182:180-187.

[17] Yang Z, Ren X, Liu Y. N-halamine modified ceria nanoparticles: Antibacterial response and accelerated wound healing application via a 3D printed scaffold. *Composites Part B-Engineering*. 2021; 227:109390(1-10).

[18] Liang X, Chen X, Zhu J, et al. A simple method to prepare superhydrophobic and regenerable antibacterial films. *Materials Research Express*. 2020;7(5):055307(1-12).

[19] Sahariah P, Cibor D, Zielinska D, et al. The Effect of Molecular Weight on the Antibacterial Activity of N,N,N-Trimethyl Chitosan (TMC). *International Journal of Molecular Sciences*. 2019;20(7):01743(1-14).

[20] Dong A, Lan S, Huang J, et al. Preparation of magnetically separable *N*-halamine nanocomposites for the improved antibacterial application. *Journal of Colloid and Interface Science*. 2011,364(2):333-340.

[21] Li R, Hu P, Ren X, et al. Antimicrobial *N*-halamine modified chitosan films. *Carbohydrate Polymers*. 2013;92(1):534-539.

[22] Tao B, Shen X, Yuan Z, et al. N-halamine-based multilayers on titanium substrates for antibacterial application. *Colloids and Surfaces B-Biointerfaces*. 2018;170:382-392.

[23] Almodovar J, Place LW, Gogolski J, et al. Layer-by-Layer Assembly of Polysaccharide-Based Polyelectrolyte Multilayers: A Spectroscopic Study of Hydrophilicity, Composition, and Ion Pairing. *Biomacromolecules*. 2011;12(7):2755-2765.

[24] Bu D, Zhou Y, Yang C, et al. Preparation of quaternarized *N*-halamine-grafted graphene oxide nanocomposites and synergetic antibacterial properties. *Chinese Chemical Letters*. 2021;32(11):3509-3513.

[25] Chang J, Yang X, Ma Y, et al. Alkyl Substituted Hydantoin-Based N-Halamine: Preparation, Characterization, and Structure-Antibacterial Efficacy Relationship. *Industrial & Engineering Chemistry Research*. 2016; 55(35):9344-9351.

[26] Bi S, Qin D, Wang T, et al. Effects of reaction environments on the structure and physicochemical properties of chitosan and its derivatives. *Carbohydrate Polymers*. 2023; 301:120357(1-11).

[27] Sahariah P, Masson M. Antimicrobial Chitosan and Chitosan Derivatives: A Review of the Structure-Activity Relationship. *Biomacromolecules*. 2017;18(11):3846-3868.

[28] Xu T, Xin M, Li M, et al. Synthesis, characterization, and antibacterial activity of N,O-quaternary ammonium chitosan. Carbohydrates Research. 2011;346:2445-2450.

[29] He J, Soderling E, Osterblad M, et al. Synthesis of Methacrylate Monomers with Antibacterial Effects Against *S. Mutans*. *Molecules*. 2011;16(11): 9755-9763.

[30] Chen Y, Feng C, Chen Q, et al. Novel composite unit with one pyridinium and three N-halamine structures for enhanced synergism and superior biocidability on magnetic nanoparticles. *Colloids and Surfaces B-Biointerfaces*. 2020;190:110890(1-10).

[31] Akdag A, McKee ML, Worley SD. Mechanism of Formation of Biocidal Imidazolidin-4-one Derivatives: An Ab Initio Density-Functional Theory Study. *Journal of the American Chemical Society*. 2006;110:7621-7627.

[32] Chen Y, Wang Y, Feng C, et al. Novel quat/di-*N*-halamines silane unit with enhanced synergism polymerized on cellulose for development of superior biocidability. *International Journal of Biological Macromolecules*. 2020;154:173-181.

[33] Yan X, Jie Z, Zhao L, et al. High-efficacy antibacterial polymeric micro/nano particles with N-halamine functional groups. *Chemical Engineering Journal*. 2014;254:110890(1-10).